Plasticity Induced Crack Closure in Adhesively Bonded Joints under Fatigue Loading

M.J. Donough[1], A.J. Gunnion[2], A.C. Orifici[1] and C.H. Wang[1*]

[1] *Sir Lawrence Wackett Aerospace Research Centre, School of Aerospace, Mechanical and Manufacturing Engineering, RMIT University, GPO Box 2476, Melbourne, Victoria 3001, Australia*
[2] *CRC-ACS, 1/320 Lorimer Street, Port Melbourne, Victoria 3207, Australia*

Keywords: Fatigue Debonding, Crack Closure, Bonded Joints

Abstract

The mean load of fatigue load cycles has a large effect on the fatigue crack growth rates in metallic materials and bonded joints. In metallic structures, this effect has been attributed to plasticity-induced crack closure, but little is known about the mechanism responsible for this mean load effect on fatigue crack growth in adhesively bonded joints. This paper presents a computational investigation of the plasticity-induced crack closure mechanism affecting disbond growth in adhesively bonded joints under fatigue loading. The results show that the ratios of crack-opening and crack-closure are approximately independent of the level of plastic constraint measured by the ratio between plastic zone size and adhesive thickness. An effective strain-energy release rate parameter, which accounts for the crack closure behaviour, has been developed as a new correlating parameter for disbond growth. Comparisons with the experimental results pertinent to four different adhesive bonded joints reveal that this new correlating parameter is capable of unifying the fatigue growth rates by eliminating the effect of mean loads.

1. Introduction

Adhesive bonding is the preferred method of joining and repairing metallic and composite structures due to several advantages over mechanical fasteners, such as improved mechanical performance. With increased confidence from successful applications and the maturity of this

[*] Correspondence author: C. H. Wang *Tel: +61 3 99256115, e-mail: chun.wang@rmit.edu.au*

technology, adhesive bonding is now widely employed in joining and repairing composite structures, including aircraft primary structures. However, the certification of adhesive bonding for field-repair of safety-critical structures remains a challenge due to concerns over their long-term durability. FAA Advisory Circular 20-107B mandates that composites and bonded structures must be designed for no growth or slow-growth to ensure continuous airworthiness [1]. A bonded repair or joints should be able to sustain the design ultimate strength in the presence of detectable disbond. Therefore validated design methodologies are required to satisfy the regulatory requirements for cyclic fatigue loading in order to implement adhesive bonding in primary structures. Fatigue crack growth in bonded joints is conventionally characterised by the strain energy release rate (SERR). However there is no consensus regarding the definition of the correlating parameter under varying load ratio where the load ratio is given as: $R = P_{min}/P_{max}$.

The most prevalent definition found in literature is the maximum strain energy release rate G_{max} [2-5] and the cyclic strain energy release rate $\Delta G = G_{max} - G_{min}$ [5-9]. More recently, a different definition of the SERR range, in keeping consistent with similitude principle as the use of ΔK for metals fatigue, has been proposed for delamination growth in composite structures [10, 11]. Mean loads have been experimentally observed to significantly affect the fatigue lives of bonded joints in a deleterious manner [7, 12, 13]. All the correlating parameters presently used will require empirical calibration to account for mean load effects in the fatigue behaviour of bonded joints. A review of the fatigue models used for fatigue debonding or delamination is covered in [14], highlighting the variety of empirical models proposed by researchers over the years. The existing empirical method of curve fitting disbond growth rates under different stress ratios renders it difficult to predict fatigue behaviour under variable amplitude or spectral loading, as evidenced by the similar problem in fatigue of metallic structures. Moreover, when the disbond growth rates are plotted in terms of the conventional definition of strain-energy release rates, increases in mean loads would result in slower growth rates, which is contradicting to experimental evidence of short fatigue lives under high mean loads [15, 16]. Therefore

a new correlating parameter is needed to correctly account for the effects of mean loads and to enable predictions of fatigue lives under variable amplitude loading conditions, overcoming the limitations of existing methods.

Since its discovery by Elber [17], plasticity-induced crack closure is now a widely accepted model to explain and account for the effects of mean loads on the cyclic crack growth behaviour in metallic materials [18-21]. Essentially crack closure reduces fatigue crack growth rates by reducing the effective stress range experienced at the crack tip. This concept has enabled the development of practical life prediction methods of metallic structures under variable spectrum loading. By contrast, very little research has been reported in the literature on the crack closure phenomenon in adhesively bonded structures.

The aim of this paper is to investigate the mechanism of plasticity-induced crack closure in bonded joints and its relationship with the effects of mean loads on disbond growth rates. A review of existing definitions of SERR range is first presented to highlight the problems in accounting for the effects of load ratio on disbond growth. Computational modelling is then performed to quantify the effect of plastic-wake induced closure on the growth behaviour of disbonds, in which the adhesive layer is modelled as a constrained layer [22, 23] undergoing elastic-plastic deformation. Based on the numerical results, a new correlating parameter is proposed, which has shown to significantly improve the correlation with experimental results of fatigue debonding under Mode I loading.

2. Review of Fatigue Crack Growth Correlating Parameter

2.1. Mode I crack growth

Based on the analogy of the Paris relation for fatigue crack growth in metals, fatigue debonding rates of bonded joints have been conventionally plotted on a log-log scale against the strain energy release rate, resulting in typical power-law relationships. In this context, two different parameters, the maximum strain energy release rate G_{max} and the cyclic strain energy release rate ΔG, have been most commonly employed to correlate the fatigue disbond growth rates:

$$\frac{da}{dN} = C_1 \left[G_{I,\max} \right]^{m_1} \tag{1}$$

$$\frac{da}{dN} = C_2 \left[\Delta G_I \right]^{m_2} \tag{2}$$

where $\Delta G_I = G_{I,\max} - G_{I,\min}$ for R > 0. Under negative load ratios (R < 0), no reports could be located in the literature on pure mode I fatigue behaviour; hence there is no consensus on the definition of ΔG_I for R < 0. The parameters, C_1, C_2, m_1, and m_2 depend on load ratio R, so they are not truly material properties. The strain energy release rate G is calculated using the Irwin-Kies relation,

$$G = \frac{P^2}{2b} \frac{\partial C}{\partial a} \tag{3}$$

where b is the specimen width and C is the compliance of specimen given as displacement divided by applied load. When fatigue crack growth rates are plotted in terms of $G_{I,\max}$, a strong dependency on load ratio has been reported [5, 15, 24]. This behaviour is not unexpected, given that the cyclic load range, which is not considered in this definition, plays a critical role in disbond growth under fatigue loading. In order to predict this load ratio dependency behaviour, past research had proposed a number of empirical expressions to determine the Paris law parameters for various load ratios by making certain assumptions about the fatigue behaviour [15, 24]. However extensive experimental testing is still required to calibrate these parameters to obtain a good fit.

The SERR range, ΔG_I, attempts to address the load ratio dependency of $G_{I,\max}$ by defining the SERR range, similar to which ΔK is defined in metal fatigue. However, it should be pointed out that the existing definition of ΔG_I is inconsistent with ΔK because $\Delta G \neq \Delta K^2 / E$, as shown below,

$$\Delta G_I \equiv \frac{K_{\max}^2 - K_{\min}^2}{E} = \frac{2K_{mean}\Delta K}{E} \neq \frac{\Delta K^2}{E} \tag{4}$$

The fundamental concept of similitude in fatigue implies that the crack-tip deformation and, hence, crack increment per cycle is uniquely controlled by a single loading parameter such as the stress intensity factor as in the case of metals [10, 25]. Considering a growing crack under constant amplitude loading, a cyclic plastic zone forms at the crack tip and a plastic wake is left behind as the crack advances. If the plastic zone is sufficiently small and within the elastic singularity zone, the crack tip condition is uniquely defined by the stress intensity factor, since the similitude condition prevails. In keeping consistent with the Irwin relationship, the cyclic SERR range $\Delta G_{I,eq}$ [10] should be defined such as that $\Delta G = \Delta K^2 / E$. Consequently the following definition for $\Delta G_{I,eq}$ will be employed in this investigation, given as: -

$$\Delta G_{I,eq} = \left(\sqrt{G_{I,\max}} - \sqrt{G_{I,\min}}\right)^2 = G_{I,\max}(1-R)^2 \qquad (5)$$

The above cyclic SERR range $\Delta G_{I,eq}$ has been reported to be a better correlating parameter than ΔG_I [10, 11]. Hojo *et al*. adopted ΔK to describe the fatigue delamination growth in composite laminates, but did not consider whether ΔG was a suitable correlating parameter [26]. Moreover fractography analysis did not indicate any signs of fibre bridging which can affect the crack propagation rates. Rans et al. [10] presented the $\Delta G_{I,eq}$ definition to be used for mode I composite delaminations. He highlighted the potential misinterpretations of delamination growth behaviour if the underlying assumptions behind the two definitions were not understood.

The experimental results of the mode I fatigue disbond growth data of four epoxy-based adhesives, taken from the literature, are plotted in Figure 1 in terms of ΔG. It can be seen in Figure 1(a) that the load ratio has negligible effects on the disbond growth rates for the results from [5]. However the disbond growth rates and threshold SERR values from [4, 7, 8], as shown in Figure 1(b-d), exhibit strong dependency on the load ratio. The threshold SERR refers to the value at which the disbond growth rate is less than 10^{-6} mm/cycle. Moreover, the load ratio dependency in Figure 1(b) and Figure

1(d) appears to be counter-intuitive: higher mean load appears to reduce debonding rates under the same ΔG. These results contradict completely with the experimental observations that higher mean stress would lead to shorter fatigue lives [7, 12]. It is also worth noting that experimental results [27-29] confirmed that disbond growth rates were slightly influenced by the bondline thickness. This influence has always been attributed to the constraint of plasticity by the stiffer substrates. Jablonski attempted to quantify the bondline thickness effect on the fatigue growth rates with crack closure [29]. By measuring the crack opening displacement locally behind the crack tip, he detected non-linearity in the compliance and was able to merge the fatigue growth rates of the two different bondline thicknesses into one narrow band.

Re-analysing the experimental data presented in Figure 1 using the $\Delta G_{1,eq}$ defined in Equation (6), shows that a lower load ratio yields higher threshold and lower debonding growth rates, as presented in Figure 2. This trend is similar to the observations of metals' fatigue behaviour. Therefore, the equivalent SERR definition is consistent with the similitude requirements in fatigue. The counter-intuitive behaviour, previously observed when ΔG was employed as the correlating parameter, has now been eliminated.

Under mode II loading, the correlating parameter ΔG is unable [30] to account the fatigue disbond growth rates for $R \geq 0$ and $R < 0$. As demonstrated in [30], the G_{max} and G_{min} terms cancel itself out at R = -1 in the ΔG definition, rendering it meaningless. Consequently a separate definition of ΔG has to be used under negative R. This particular example reiterates the flaw in the definition of ΔG.

Nakagaki and Alturi conducted numerical crack growth analysis of mixed-mode fatigue crack growth in isotropic materials [31] and reported no crack closure under pure mode II loading. The absence of crack closure in mode II can be attributed to that cyclic deformation occurs parallel to the fracture plane rather than perpendicular to it. In the absence of plasticity induced crack closure under mode II loading, the load ratio dependency of mode II fatigue disbond growth rates can be eliminated by using ΔG_{eq} as the correlating parameter [10, 11]. Although friction may induce mean load

dependency behaviour, its contribution is negligible and mode II disbond growth is driven primarily by the cyclic load range.

2.2. Summary of key issues

The above section highlights the deficiencies of current scaling parameters for bonded joints based on strain energy release rates, both in terms of correlation with experimental results and consistency with the theoretical requirement of similitude. When experimental data of disbond growth rates are plotted against the equivalent strain energy release rates ΔG_{eq}, a strong load-ratio effect is clearly evident for mode I loading (referring to Figure 2); under mode II loading, the equivalent strain energy release rate is able to unify growth rates under different load ratios. Therefore, a new scaling parameter is required to correlate mode I disbond growth data.

In light of the success of the plasticity-induced crack closure concept [19] in explaining and unifying the load-ratio dependence of mode I fatigue cracks in metals, it is contended that the load-ratio effects in bonded joints are also likely caused by the plasticity-induced crack closure phenomenon. Since most structural adhesives are ductile materials capable of large plastic deformation before failure, plastic stretch of the adhesive during mode I loading will leave behind a plastic wake, just like the case of fatigue cracks in metallic materials.

The following section describes a computational simulation using the finite element method to quantify the effects of plasticity-induced crack closure on disbond growth in bonded joints subjected to fatigue loading. The results will then be employed to formulate a new correlating parameter to account for the mean load effects in bonded joints in subsequent sections.

3. Modelling of Plasticity Induced Crack Closure

3.1. Problem formulation

A study of crack closure within an adhesive layer in a joint was carried out under mode I loading. Figure 3a shows a schematic of a double cantilever beam (DCB) specimen typically used to measure the mode I fatigue debonding rates of an adhesive joint. The bonded DCB specimen consisted of a unidirectional composite substrate and an adhesive having a nominal thickness of 0.2 mm. The crack was assumed to have propagated cohesively in the middle of the bondline where $h_1 = h_2$.

There are two cases in which plasticity can occur within the bondline as shown in Figure 3b and 5c. In the first scenario, the plastic zone is sufficiently small and is contained within the bondline thickness and the crack-tip singularity zone. Therefore the small-scale yielding condition is satisfied; this case is denoted as un-constrained plasticity. In the second scenario, the plastic zone extends to the adherends and is entirely bounded within the adhesive layer. This condition is denoted as constrained plasticity.

Applying the von Mises yield criterion, the shape of an unconstrained plastic zone can be analysed and derived as a function of θ. Hence the boundary of a plane strain plastic zone is given as:

$$r_1(\theta) = \frac{K_{\max}^2}{4\pi\sigma_y^2}\left[\frac{3}{2}\sin^2\theta + (1-2\upsilon)^2(1+\cos\theta)\right] \tag{6}$$

where σ_y and $K_{\max}$ denote the adhesive's yield strength and the maximum applied stress intensity factor. In the case of a crack within a constrained layer [22, 23], the maximum stress intensity factor is related to the applied strain energy release rate via the usual relationship $K_{\max} = \sqrt{G_{\max} E_A}$, with E_A being the Young's modulus of the adhesive.

Figure 3d shows the shape of the unconstrained, plane strain plastic zone, derived from equation (6) normalised by the Irwin's plastic zone length approximation in plane strain. The plastic zone height r_y, on either side of the crack tip is given in equation (7). The forward plastic zone length r_x is approximately given when $\theta \approx \pi/4$.

$$r_y = r_1\left(\frac{\pi}{2}\right) = 1.15\left[\frac{1}{3\pi}\frac{E_A G_{max}}{\sigma_y^2}\right] \quad (7)$$

$$r_x \approx r_1\left(\frac{\pi}{4}\right) \approx 0.5\left[\frac{1}{3\pi}\frac{E_A G_{max}}{\sigma_y^2}\right] \quad (8)$$

The case of constrained plasticity is defined when r_y is equal or greater than $t_A/2$.

3.2. Modelling Methodology

In metal fatigue, numerical analyses have been successfully employed to simulate fatigue crack growth and closure to quantify the effect of load ratio on the rate of crack growth [32]. In this work we will employ the finite element method to quantify the plasticity-induced crack closure in an adhesively bonded joint, adapting the modelling guidelines developed for cracks in isotropic materials as discussed in Refs [32-36]. The two parameters that may affect the numerical results are the crack advance length and the total crack growth length. The crack advance length is herein equal to the element length. The total crack growth length is associated to the development of the plastic wake and has a direct influence on the opening and closing loads. In order to develop a robust numerical model, it is crucial to consider the numerical disbond growth process; i.e. crack tip element size, the development of the plastic wake, load cycle and crack propagation process.

Computational simulations of a DCB specimen were performed using Abaqus Standard solver in a multi-step analysis. Only half the specimen was modelled due to symmetry. Four noded, quadrilateral plane-strain elements (CPE4) were used to model the entire specimen. The elements in the vicinity of the crack tip and along the crack propagation had an aspect ratio of one for better precision due to the high strain gradients. The transition from a coarse mesh to a fine mesh at the crack tip is presented in Figure 4. The forward horizontal plastic zone r_x (equation 8) is used as a reference length in the mesh refinement studies to ensure sufficient elements are used to represent the reversed plastic

zone, as recommended by [33, 36]. The crack tip elements lengths, l_e, were varied from 0.001 mm to 0.0025 mm depending on the applied load.

The composite substrates consisted of 12 unidirectional plies made of T300/5208 carbon epoxy prepregs, with ply thickness after cure being 0.13 mm. The substrate was assumed to remain elastic throughout the cyclic loading. The bondline was given the properties of EC-3445 adhesive. The von Mises yield criterion was employed to model the plastic yielding of the adhesive. The material input properties of the numerical simulation are given in Table 1.

The specimen was cyclically loaded under load control at constant amplitude as summarised in Figure 5. Crack propagation was achieved by liberating the crack tip node from its constraint by changing boundary conditions between successive analysis steps. Although there is no universal rule governing at what instance of the load cycle a node should be released, the most accepted practice [32, 33, 35] is to advance the crack at P_{max} due to it having a greater physical sense (the higher stress at the crack tip, the more likelihood of crack growth). Previous work has indicated that the influence of the nodal release at any point of the loading cycle takes place is minimal, provided sufficient mesh density is used [35]. Since the actual unzipping and opening of the crack is a continuous process, a numerical stabilisation step was carried out to approximate this process. At the start of the step (e.g. step no. 2 in Figure 5), the boundary condition ($u_y = 0$) at the crack tip is removed. The node will nonetheless remain closed and the boundary condition is replaced with a nodal force to maintain equilibrium. Therefore a constant, peak load was applied to the model. Subsequently, the node is released and its nodal reaction forces equals to zero prior to the unloading step. It is reported that the influence of the plastic wake on closure is far less under plane strain than under plane stress due to the small area which closure occurs [33, 35]. Hence the crack length is allowed to propagate 25 times the crack tip element length in order to propagate it past the initial monotonic plastic zone.

The contact of crack faces was simulated by placing a rigid body at the crack plane and employing a hard contact interaction to prevent the nodes from inter-penetrating in the event of closure. Crack closure was determined with either the nodal contact criterion or crack-tip stress criterion during

a loading cycle. The nodal contact criterion defines crack closure load as when the nodes just behind the crack tip make contact during unloading, which has been commonly used in the simulation of plane stress crack closure [35]. When the vertical nodal displacement becomes positive, the crack surface is then interpreted as open and the corresponding load is defined as the crack opening load.

The second crack closure definition used in this paper employs a stress-based criterion taken at the crack tip node, as proposed by Sehitoglu and Sun [34] and Wu and Ellyin [37]. This criterion is based on the premise that crack propagation cannot occur under compressive stress fields behind and ahead of the crack tip since the nucleation of micro-cracks is a strongly dependent on tensile stresses. The crack opening load is defined when the nodal forces at the crack tip overcomes the compressive stress during the loading segment of the load cycle. The crack closure load is defined as when the nodal forces changes from tension to compression during unloading. The crack tip stress criterion has facilitated the crack closure analysis under plane strain where contact can be difficult to evaluate. While the displacement of the node immediately behind the crack tip may become positive, contact of the crack flanks may still occur between the crack tip and this node [37]. As only a small area of the plastic wake comes into contact under plane strain conditions, this makes the results, based on nodal contact, difficult to assess.

3.3. Results

The strain energy release rate of the DCB specimen was determined analytically using corrected beam theory and is expressed by means of the following expression.

$$G_I = \frac{12P^2(a+\chi h)^2}{E_{11}b^2h^3} \tag{9}$$

where

$$\chi = \left(\frac{E_{33}}{11G_{13}}\right)^{1/2}\left[3-2\left(\frac{\Gamma}{1+\Gamma}\right)^2\right]^{1/2}$$

$$\Gamma = \frac{1.18\left(E_{33}G_{13}\right)^{1/2}}{G_{13}}$$

A mesh refinement study on the crack closure behaviour of the DCB model was conducted to ensure an appropriate crack tip element size was used in the following analyses. The resolution of the crack tip mesh is defined by the crack tip element length, l_e, normalised by the plastic zone length r_x, given in equation (8). The results of the mesh refinement study using either the crack tip stress criterion or the nodal contact criterion are shown in Figure 6a and 6b respectively. A lack of convergence was observed for the closing loads for both criteria. Consequently, a unique solution cannot be obtained based solely on the closing loads. The crack opening loads, however, is seen to show converging behaviour as l_e/r_x approaches 0.1. It should be noted that further refinement of the crack tip mesh beyond $l_e/r_x = 0.1$ causes significant element distortion, rendering the numerical results invalid. Such behaviour was reported by [36, 38] for a plane-strain compact tension model. Potential explanations for this include plane-strain locking and excessive plastic deformations. Therefore the crack tip mesh size used in the following analyses is maintained to give $l_e/r_x > 0.1$.

The following analysis investigated the influence of load ratio on the crack closure behaviour in a bonded DCB joint. The load ratio is an important parameter as a result of the influence of the minimum load in the developing plastic wake. At the given bondline thickness and l_e/r_x, the plastic zone height r_y is considerably smaller than the bondline thickness. Therefore small scale yielding conditions is valid. Several empirical closed form expressions have been proposed by different researchers to represent the load ratio effect on crack closure in metals. Newman's analytical estimate of crack opening stress was used to compare with the numerical results [39]. The following equations were fitted to the crack opening stresses from the numerical simulation of a centre crack tension specimen:-

$$\frac{\sigma_{op}}{\sigma_{\max}} = \begin{cases} A_0 + A_1 R + A_2 R^2 + A_3 R^3 & \text{for } R \geq 0 \\ A_0 + A_1 R & \text{for } -1 \leq R < 0 \end{cases} \qquad (10)$$

where

$$A_0 = 0.825 - 0.34\alpha + 0.05\alpha^2$$

$$A_1 = 0$$

$$A_2 = 1 - A_0 - A_1 - A_3$$

$$A_3 = 2A_0 + A_1 - 1$$

The comparisons of crack closure behaviour in a bonded joint and isotropic (E_S = E_A) DCB specimen are shown in Figure 7. The crack closure level of the bonded joint based on nodal contact criterion coincides with Newman's analytical solution for α = 3. The crack opening loads given by the nodal contact criterion is lower than the crack tip stress criterion. Under plane-strain conditions, since the plastic wake extends to a small area as indicated by McClung [33], the use of displacement criterion can lead to large fluctuations in the crack opening loads. At higher load ratios, further mesh refinement is needed to accurately evaluate the crack opening loads by the nodal contact criterion. However this leads excessive deformation at the crack tip element and other issue mentioned earlier. Hence the nodal contact results may not be reliable. Moreover numerical studies done by Newman et al. [20] showed that a constraint factor of 1.73 is more representative an actual structure.

When the crack-tip stress criterion was used, the crack opening loads of bonded joints are closer to the analytical solution for α = 1.73. The crack opening loads of a crack in an isotropic DCB is approximately the equivalent to the crack opening loads of a bonded DCB. Therefore it is reasonable to conclude small-scale yielding conditions are valid for fatigue loads in a bonded DCB. No closure was observed at load ratio above 0.7. Under negative load ratios, the crack opening loads remain constant at the same level when R=0 for the isotropic DCB. Therefore the crack closure behaviour of negative R can be simplified into as the crack flanks undergoing compressive stresses due to contact in this case. For the bonded joints, the crack opening values decreases slightly under negative R.

In the event of constrained plasticity, the crack opening loads of the bonded DCB specimen was investigated to determine any changes in its behaviour when small scale yielding conditions may not be valid. The substrate thickness and applied load were kept constant at 1.56 mm and l_e/r_x = 0.1 respectively. Constrained plasticity is defined when the unconstrained plastic zone height is greater than the bondline thickness, given as $2r_y/t_A \geq 1$. The results of the crack opening loads with respect to

changes in the bondline thickness are presented in Figure 8. The results based on the nodal contact criterion shows a gradual increase in the crack opening values as the level of constraint increases. In using the nodal stress criterion, the crack opening loads were observed to remain independent of the bondline thickness at R = 0 and 0.5. The slight scatter in the crack opening load results is likely due to the numerical inaccuracy in the finite element calculations. Therefore the nodal stress criterion may represent a better option than the nodal contact criterion for bonded joints as its results are independent of the level of constraint within the adhesive.

4. A New Correlating Parameter

The crack closure concept is used to characterise the load ratio dependency behaviour observed in the mode I fatigue disbond propagation in bonded joints when similitude conditions are maintained. Based on the numerical results presented in the previous section, correlating parameters are defined as shown in Equation (11). The crack opening loads are defined using the crack tip stress criterion.

$$\Delta G_{eff} = \left(\sqrt{G_{I,\max}} - \sqrt{G_{I,op}}\right)^2 = G_{I,\max}\left(1 - \frac{P_{op}}{P_{\max}}\right)^2 = \Delta G_{I,eq} U^2 \qquad (11)$$

where the parameter U denotes the effective load range ratio,

$$U = \frac{\Delta P_{eff}}{\Delta P} = \frac{P_{\max} - P_{op}}{P_{\max} - P_{\min}} = \frac{1 - P_{op}/P_{\max}}{1 - R} \qquad (12)$$

It is worth noting that the relationship given by equation (11) is consistent with the definition of effective stress intensity factor range $\Delta K_{eff} = U\sqrt{\Delta G_{I,eq} E}$. In Figure 9, the effective load range ratio U of bonded joints, according to the numerical results from the finite element modelling, are better correlated to the analytical solution of $\alpha = 1.73$ for $R \leq 0$. At increasing positive R, the numerical results of U is between the analytical solution of $\alpha = 1$ and 1.73. Although at load ratio between 0.3 and 0.6, the results are better correlated with $\alpha = 1$.

To provide an approximate, closed form expression for the effective load range ratio *U* of a bonded joint, the numerical results in Figure 9 are curve fitted using a cubic expression and is given below,

$$U = A_0 + A_1 R + A_2 R^2 + A_3 \mathrm{R}^3 \qquad for\ -1 \geq R \geq 1 \tag{13}$$

where

$A_0 = 0.56$

$A_1 = 0.3$

$A_2 = 0.19$

$A_3 = 0.12$

This expression furnishes a convenient solution for bonded joints subjected to fatigue loading. The results of using ΔG_{eff} to quantify the mean load dependency, previously observed with ΔG_{eq}, are plotted in Figure 10. The fatigue growth data in Figure 10b and 10d can be collapsed into a narrow band whereas Figure 10a and 10c still display a substantial load ratio dependency behaviour.

Although the Paris model took account of the effective load ratio induced by crack closure, it cannot account for the instability of the crack growth when the applied load approaches its critical fracture value. To this end, the Forman model [40] offers a simple correction to account for the influence fracture toughness on the fatigue crack growth curve. Extending the Forman model in terms of SERR yields

$$\frac{da}{dN} = \frac{C_F (\Delta G_{I,eff})^{m_F}}{(1-R)\left(\sqrt{G_C} - \sqrt{G_{\max}}\right)} \tag{14}$$

where G_C is the fracture toughness of the adhesive and C_F and m_F are the material constants derived from the Forman model. At each experimental data point, the modified Forman equation, as discussed in [41], represents data at various load ratios by computing the factored rate of disbond growth

$$Q = (1-R)\left(\sqrt{G_C} - \sqrt{G_{\max}}\right)\frac{da}{dN} \tag{15}$$

Comparing Equation (15) and (16), the modified Forman equation can then be represented as

$$Q = C_F \left(\Delta G_{eff} \right)^{m_F} \tag{16}$$

The fatigue crack growth data of the four adhesives considered in this study are plotted using the modified Forman equation and the results are shown in Figure 11. The critical SERR value G_C of the adhesives are reported in [4, 16, 27, 42] The Forman model is able to collapse the fatigue growth trends into a narrow band. A single threshold SERR value can also be obtained for which a bonded joint or repair can be designed to satisfy the no-growth criterion.

It can now be concluded that the new correlating parameter, which accounts for load ratio effect using plasticity-induced crack closure concept, is able to unify disbond growth rates under different load ratios, making it possible to predict fatigue lives of bonded structures under variable amplitude or spectrum loadings. This new finding paves the way for applying the plasticity-induced crack closure model, with appropriate treatment of the constraints imparted by the stiff adherends, to analyse the load interactions between load cycles and developing a predictive model for determining the disbond growth in bonded joints under variable amplitude or spectrum loading.

5. Conclusions

A critical review of existing correlating parameters used for disbond growth in bonded joints under fatigue loading has revealed a significant deficiency in existing scaling parameters to provide consistent and physically correct correlation with fatigue results of bonded joints. Detailed computational modelling of the plastic wake contact showed a growing fatigue crack in a bonded joint experiences significant level of plasticity-induced crack closure, contrary to the common belief that plasticity induced crack closure is absent in bonded structures. The results of the present computational modelling showed that the level of plasticity-induced crack closure depends only on applied load ratios and is independent of the applied load levels. A new correlating parameter, defined in terms of the

effective cyclic load range, has been demonstrated to provide excellent correlation with experiment data of four different adhesives under varying load ratios.

Acknowledgements

This work was undertaken within the Robust Composite Repair project, part of a CRC-ACS research program, established and supported under the Australian Government's Cooperative Research Centres Program.

Reference

1. FAA, *Composite Aircraft Structure: Advisory Circular (AC) 20-107B*, 2010, FAA.
2. Kinloch, A.J. and S.O. Osiyemi, *Predicting the Fatigue Life of Adhesively-Bonded Joints.* The Journal of Adhesion, 1993. **43**(1-2): p. 79-90.
3. Ashcroft, I.A. and S.J. Shaw, *Mode I fracture of epoxy bonded composite joints 2. Fatigue loading.* International Journal of Adhesion and Adhesives, 2002. **22**(2): p. 151-167.
4. Hojo, M., et al., *Modes I and II interlaminar fracture toughness and fatigue delamination of CF/epoxy laminates with self-same epoxy interleaf.* International Journal of Fatigue, 2006. **28**(10): p. 1154-1165.
5. Mall, S., G. Ramamurthy, and M.A. Rezaizdeh, *Stress ratio effect on cyclic debonding in adhesively bonded composite joints.* Composite Structures, 1987. **8**(1): p. 31-45.
6. Joseph, R., et al., *Fatigue Crack Growth in Epoxy/Aluminum and Epoxy/Steel Joints.* The Journal of Adhesion, 1993. **41**(1-4): p. 169-187.
7. Erpolat, S., et al., *Fatigue crack growth acceleration due to intermittent overstressing in adhesively bonded CFRP joints.* Composites Part A: Applied Science and Manufacturing, 2004. **35**(10): p. 1175-1183.
8. Pirondi, A. and G. Nicoletto, *Fatigue crack growth in bonded DCB specimens.* Engineering Fracture Mechanics, 2004. **71**(4–6): p. 859-871.
9. Azari, S., et al., *Fatigue threshold behavior of adhesive joints.* International Journal of Adhesion and Adhesives, 2010. **30**(3): p. 145-159.
10. Rans, C., R. Alderliesten, and R. Benedictus, *Misinterpreting the results: How similitude can improve our understanding of fatigue delamination growth.* Composites Science and Technology, 2011. **71**(2): p. 230-238.
11. Matsubara, G., H. Ono, and K. Tanaka, *Mode II fatigue crack growth from delamination in unidirectional tape and satin-woven fabric laminates of high strength GFRP*. International Journal of Fatigue, 2006. **28**(10): p. 1177-1186.
12. Crocombe, A.D. and G. Richardson, *Assessing stress state and mean load effects on the fatigue response of adhesively bonded joints.* International Journal of Adhesion and Adhesives, 1999. **19**(1): p. 19-27.
13. Nolting, A.E., P.R. Underhill, and D.L. DuQuesnay, *Variable amplitude fatigue of bonded aluminum joints.* International Journal of Fatigue, 2008. **30**(1): p. 178-187.
14. Pascoe, J.A., R.C. Alderliesten, and R. Benedictus, *Methods for the prediction of fatigue delamination growth in composites and adhesive bonds – A critical review.* Engineering Fracture Mechanics, 2013. **112–113**(0): p. 72-96.

15. Andersons, J., M. Hojo, and S. Ochiai, *Empirical model for stress ratio effect on fatigue delamination growth rate in composite laminates.* International Journal of Fatigue, 2004. **26**(6): p. 597-604.
16. Erpolat, S., et al., *A study of adhesively bonded joints subjected to constant and variable amplitude fatigue.* International Journal of Fatigue, 2004. **26**(11): p. 1189-1196.
17. Elber, W., *Fatigue crack closure under cyclic tension.* Engineering Fracture Mechanics, 1970. **2**(1): p. 37-45.
18. Newman, J.C.J., *Application of a closure model to predict crack growth in three engine disc materials.* Int. J. Fracture, 1996. **80**: p. 193-218.
19. Newman, J.C.J., *FASTRAN-II: a fatigue crack growth structural analysis program,* 1982, NASA Technical Memorandum 104159,Langley Research Centre, Hampton, Virginia, USA.
20. Wang, C.H., L.R.F. Rose, and J.C. Newman, *Closure of plane-strain cracks under large-scale yielding conditions.* Fatigue & Fracture of Engineering Materials & Structures, 2002. **25**(2): p. 127-139.
21. Rose, L.R.F. and C.H. Wang, *Self-similar analysis of plasticity-induced closure of small fatigue cracks.* Journal of the Mechanics and Physics of Solids, 2001. **49**(2): p. 401-429.
22. Wang, C.H., *On the fracture of constrained layers.* International Journal of Fracture, 1998. **93**(1-4): p. 227-246.
23. Wang, C.H., *Analysis of cracks in constrained layers.* International Journal of Fracture, 1997. **83**(1): p. 1-17.
24. Shivakumar, K., et al., *A total fatigue life model for mode I delaminated composite laminates.* International Journal of Fatigue, 2006. **28**(1): p. 33-42.
25. Anderson, T.L., *Fracture Mechanics: Fundamentals and Applications*. 3 ed. 2005, Boca Raton, FL: Taylor & Francis. 640.
26. Hojo, M., et al., *Effect of matrix resin on delamination fatigue crack growth in CFRP laminates.* Engineering Fracture Mechanics, 1994. **49**(1): p. 35-47.
27. Mall, S. and G. Ramamurthy, *Effect of bond thickness on fracture and fatigue strength of adhesively bonded composite joints.* International Journal of Adhesion and Adhesives, 1989. **9**(1): p. 33-37.
28. Azari, S., M. Papini, and J.K. Spelt, *Effect of adhesive thickness on fatigue and fracture of toughened epoxy joints – Part I: Experiments.* Engineering Fracture Mechanics, 2011. **78**(1): p. 153-162.
29. Jablonski, D.A., *Fatigue Crack Growth in Structural Adhesives.* The Journal of Adhesion, 1980. **11**(2): p. 125-143.
30. Mall, S. and N.K. Kochhar, *Characterization of debond growth mechanism in adhesively bonded composites under mode II static and fatigue loadings.* Engineering Fracture Mechanics, 1988. **31**(5): p. 747-758.
31. Nakagaki, M. and S.N. Atluri, *Elastic-plastic Analysis of Fatigue Crack Closure in Modes I and II.* AIAA Journal, 1980. **18**(9): p. 1110-1117.
32. Zapatero, J., B. Moreno, and A. González-Herrera, *Fatigue crack closure determination by means of finite element analysis.* Engineering Fracture Mechanics, 2008. **75**(1): p. 41-57.
33. McClung, R.C. and H. Sehitoglu, *On the finite element analysis of fatigue crack closure—1. Basic modeling issues.* Engineering Fracture Mechanics, 1989. **33**(2): p. 237-252.
34. Sehitoglu, H. and W. Sun, *Modelling of Plane Strain Fatigue Crack Closure.* Journal of Engineering Materials and Technology, 1991. **113**(1): p. 31-40.
35. Solanki, K., S.R. Daniewicz, and J.C. Newman Jr, *Finite element analysis of plasticity-induced fatigue crack closure: an overview*. Engineering Fracture Mechanics, 2004. **71**(2): p. 149-171.
36. Solanki, K., S.R. Daniewicz, and J.C. Newman Jr, *Finite element modeling of plasticity-induced crack closure with emphasis on geometry and mesh refinement effects.* Engineering Fracture Mechanics, 2003. **70**(12): p. 1475-1489.

37. Wu, J. and F. Ellyin, *A study of fatigue crack closure by elastic-plastic finite element analysis for constant-amplitude loading.* International Journal of Fracture, 1990. **82**(1): p. 43-65.
38. González-Herrera, A. and J. Zapatero, *Influence of minimum element size to determine crack closure stress by the finite element method.* Engineering Fracture Mechanics, 2005. **72**(3): p. 337-355.
39. Newman, J.C., Jr., *A crack opening stress equation for fatigue crack growth.* International Journal of Fracture, 1984. **24**(4): p. R131-R135.
40. Forman, R.G., V.E. Kearney, and R.M. Engle, *Numerical Analysis of Crack Propagation in Cyclic-Loaded Structures.* Journal of Fluids Engineering, 1967. **89**(3): p. 459-463.
41. Tavares, S., et al. *Modeling of fatigue crack growth in monolithic integral stiffened panels taking into account residual stress*. in *Iberian Conference on Fracture and Structural Integrity*. 2010.
42. Pirondi, A. and G. Nicoletto, *Mixed Mode I/II fracture toughness of bonded joints.* International Journal of Adhesion and Adhesives, 2002. **22**(2): p. 109-117.

Table 1: Material properties used in the finite element model

Substrate : T300/5208				Adhesive : EC-3445	
E_{11} =	131000 MPa	E_{33} =	13000 MPa	E =	1810 MPa
G_{13} =	6400 MPa	G_{23} =	6400 MPa	ν =	0.4
$\nu_{12} = \nu_{13}$ =	0.35	ν_{23} =	0.34	σ_y =	58 MPa

Figures

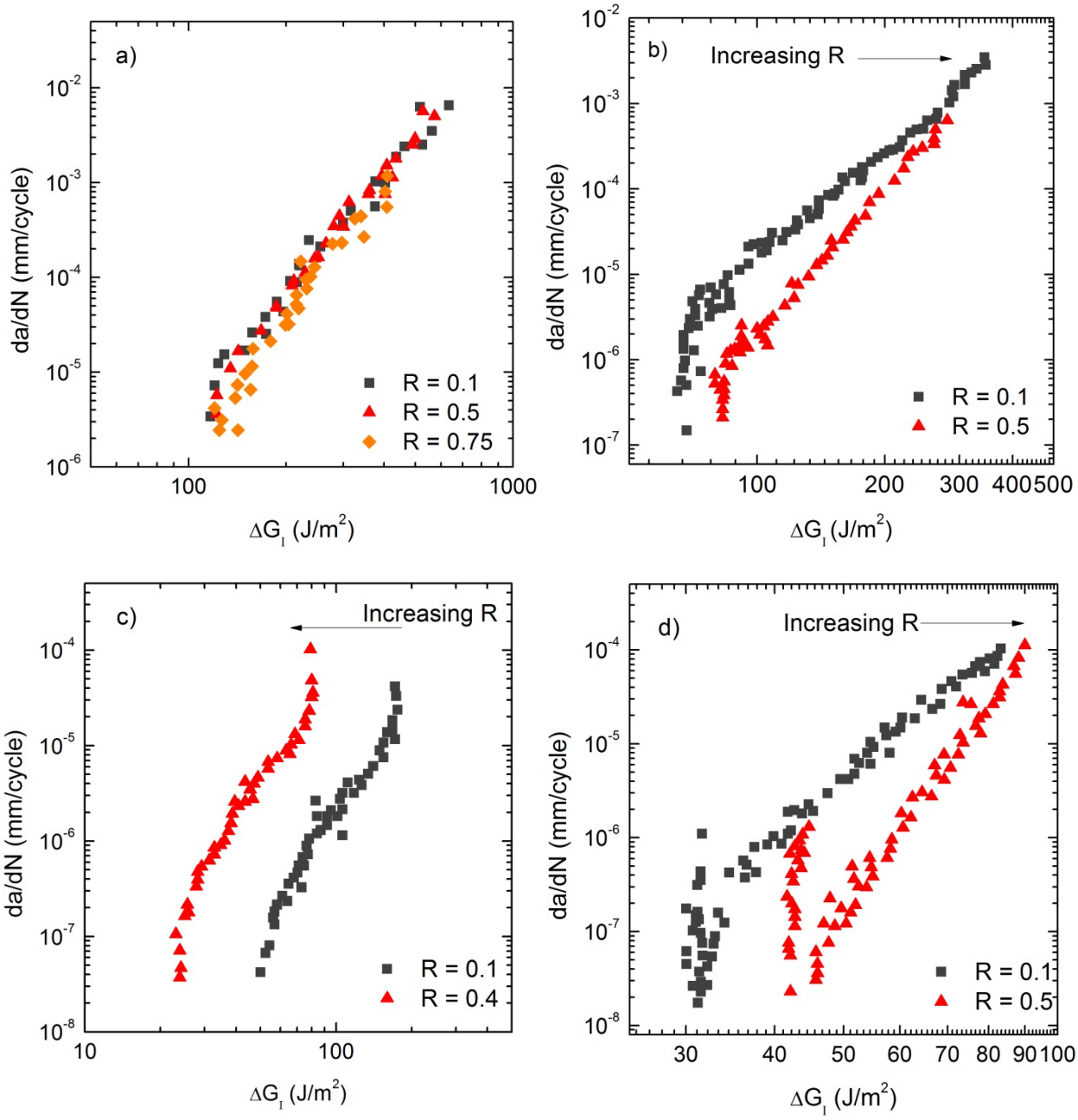

Figure 1 Experimental results of mode I fatigue debonding of a) EC-3445 [5], b) Cytec 4535A [7], c) Multibond 330 [8] and d) Toho 111 interleaved [4] adhesives versus ΔG_I

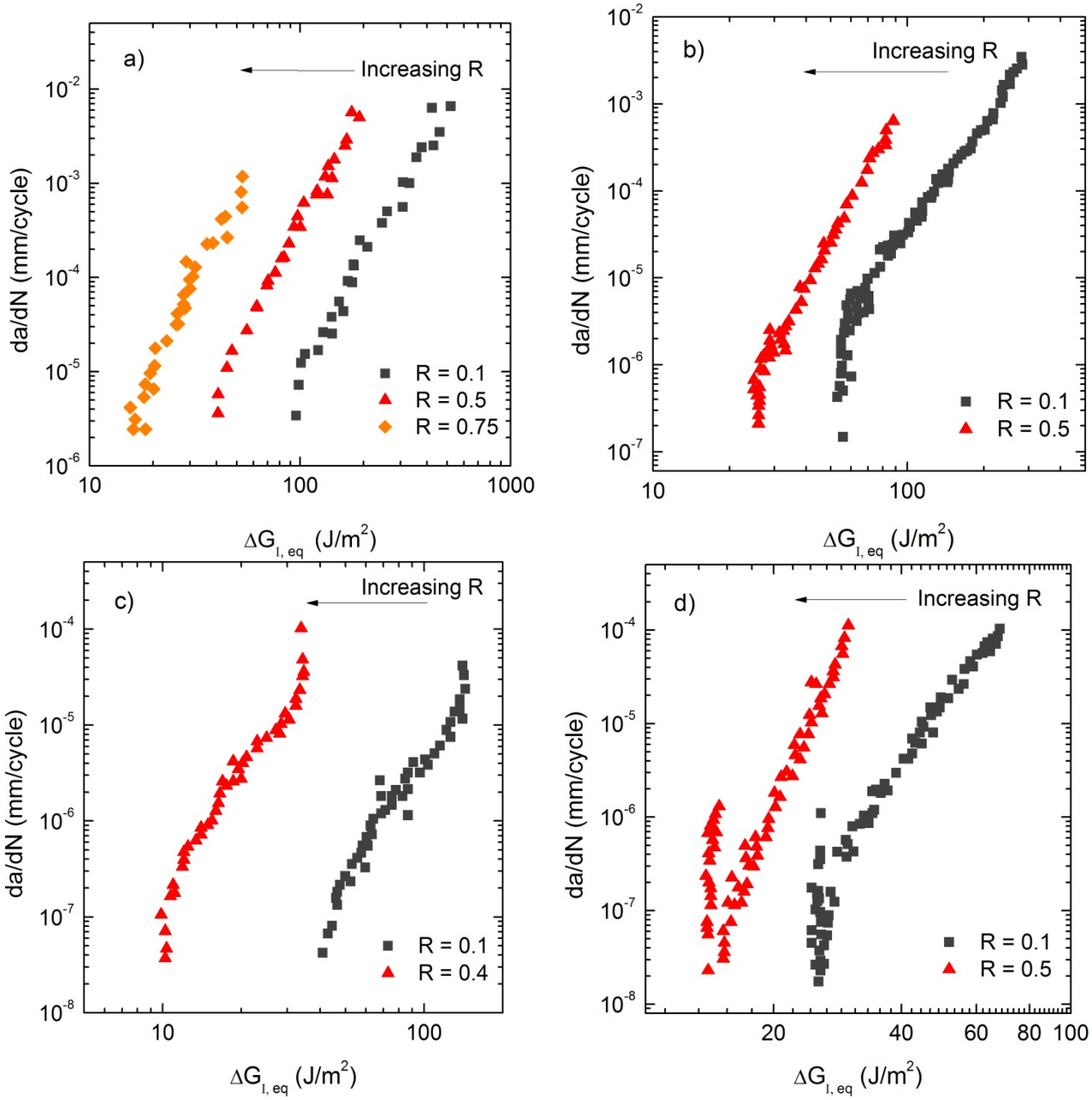

Figure 2 Mode I disbond growth rates versus equivalent strain energy release rate $\Delta G_{I,eq}$ for (a) EC-3445 [5], b) Cytec 4535A [7], c) Multibond 330 [8] and d) Toho 111 interleaved [4] adhesives.

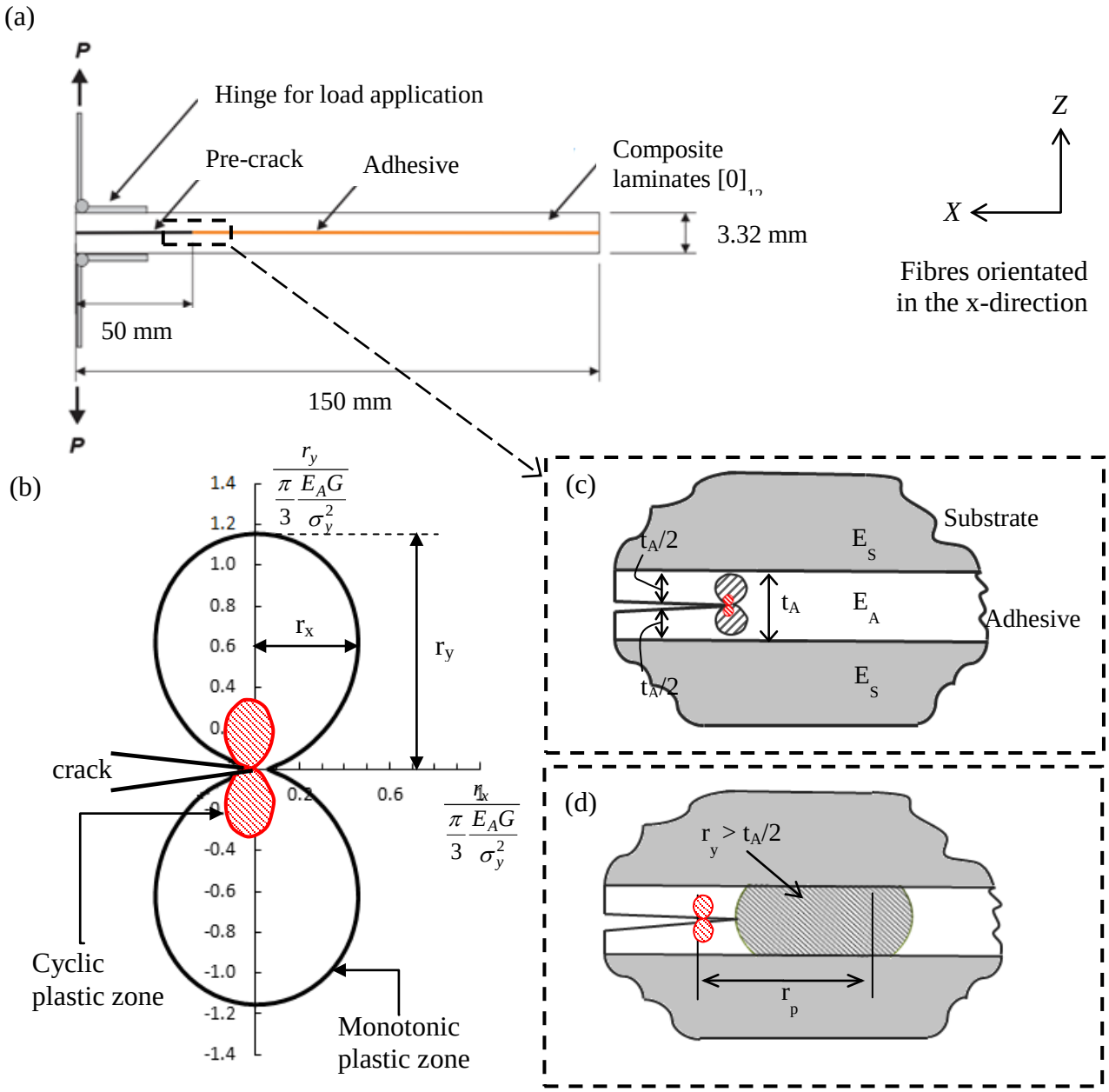

Figure 3 Schematic of (a) double cantilever bonded joint specimen, (b) unconstrained plastic deformation in an homogeneous material, (c) un-constrained plastic zone of a disbond in a bonded joint, and (d) constrained plastic zone of a disbond in a joint.

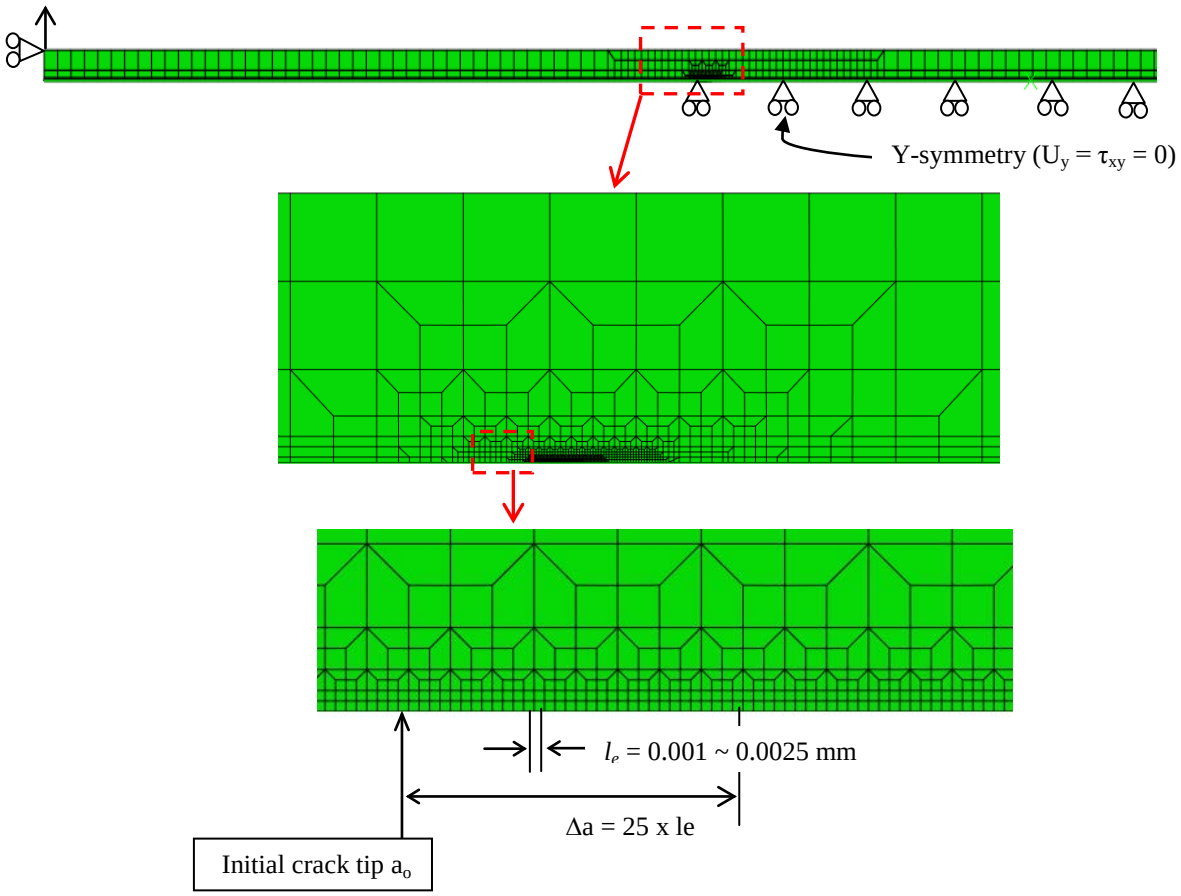

Figure 4 Finite element mesh and boundary conditions used for double cantilever bonded joint specimen

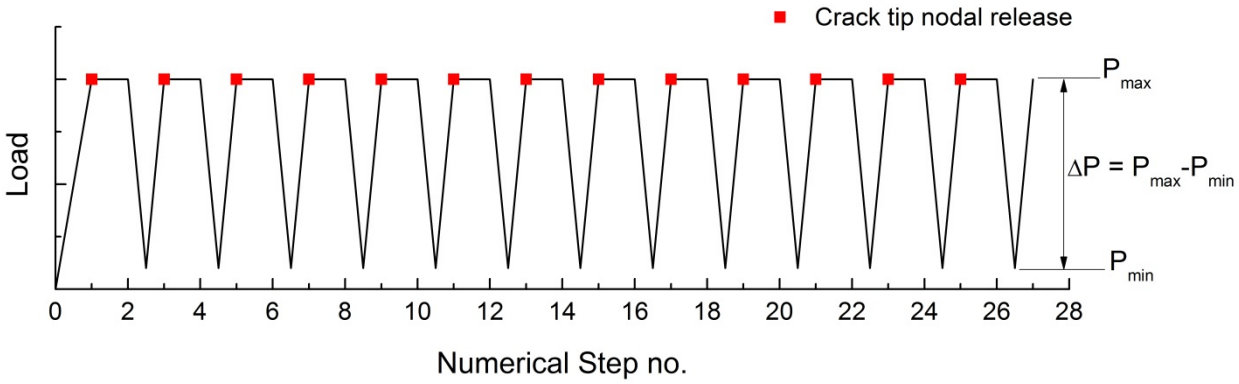

Figure 5 Numerical load history and node release scheme

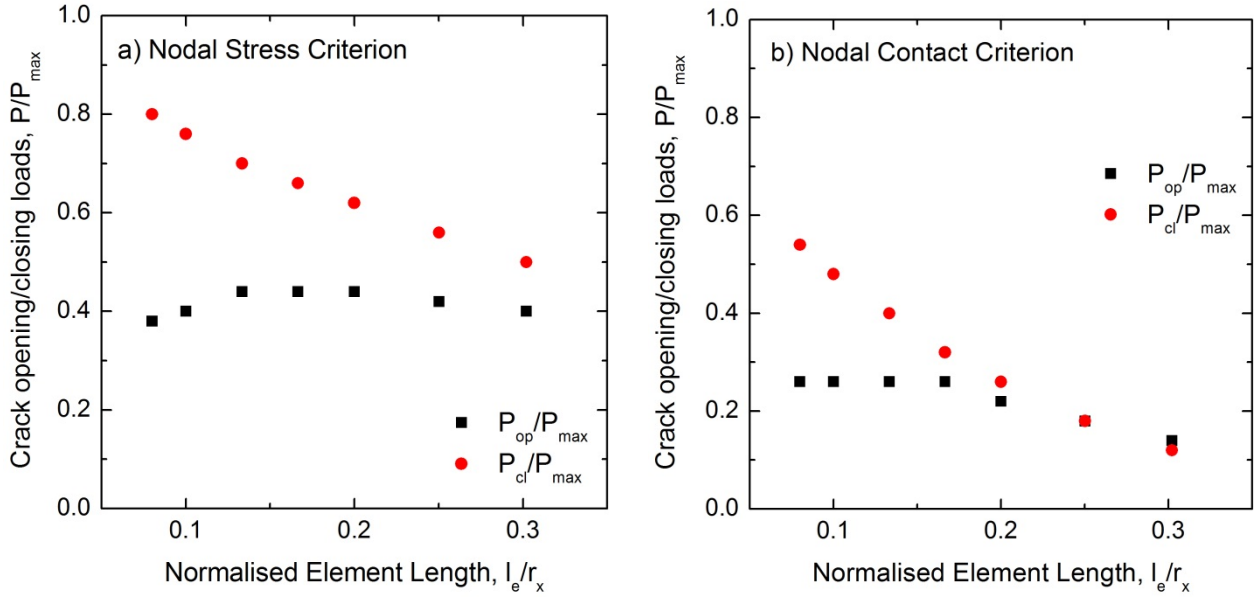

Figure 6 Effect of crack tip mesh size on the crack opening and closing values using a) crack tip nodal stress criterion and b) nodal contact criterion at R = 0

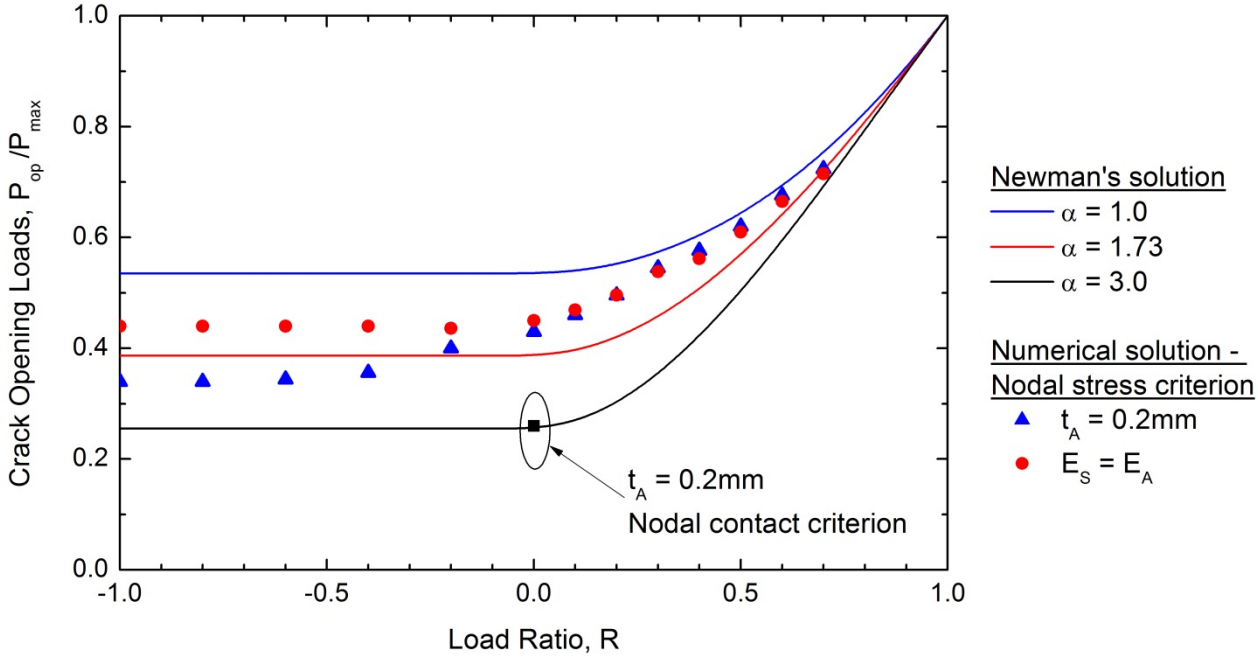

Figure 7 Influence of load ratio on the crack closure behaviour in a bonded and isotropic DCB joint specimen

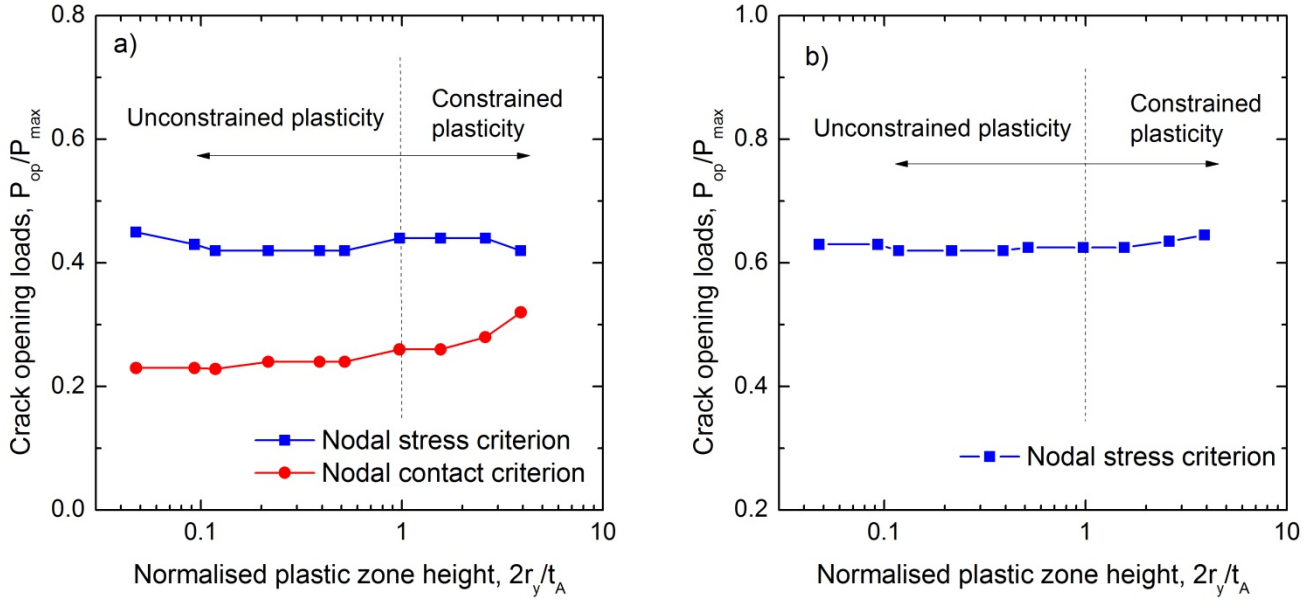

Figure 8 Influence of bondline thickness on the crack opening values at a) R = 0 and b) R = 0.5

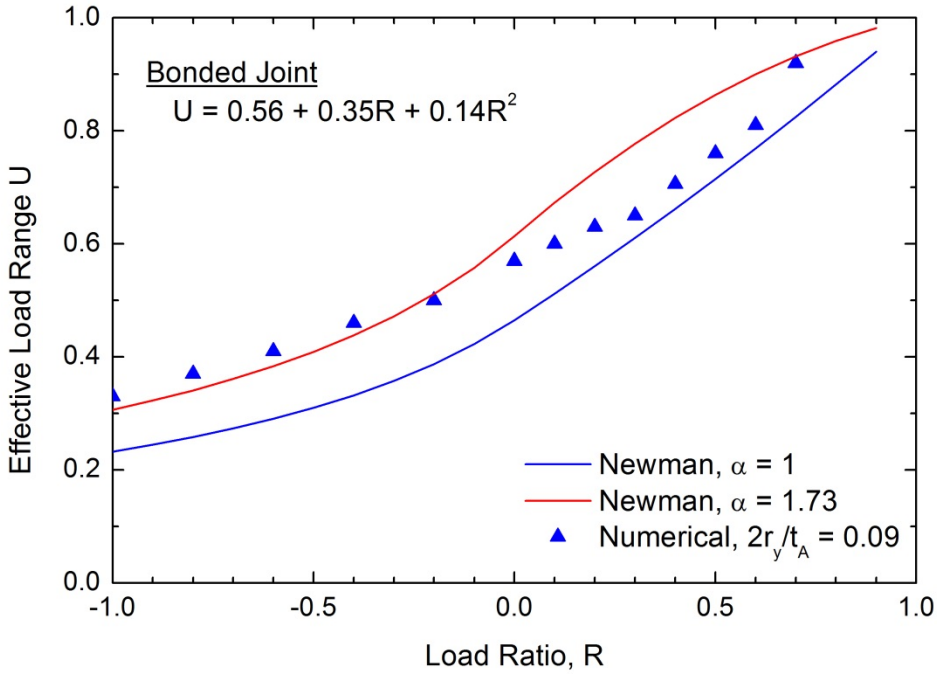

Figure 9 Effective load range ratio for a bonded DCB joint

Figure 10 Correlation of mode I fatigue debonding results with $\Delta G_{I,eff}$ for (a) EC-3445 [5], (b) Cytec 4535A [7], (c) Multibond 330 [8] and (d) Toho 111 interleaved [4] adhesives.

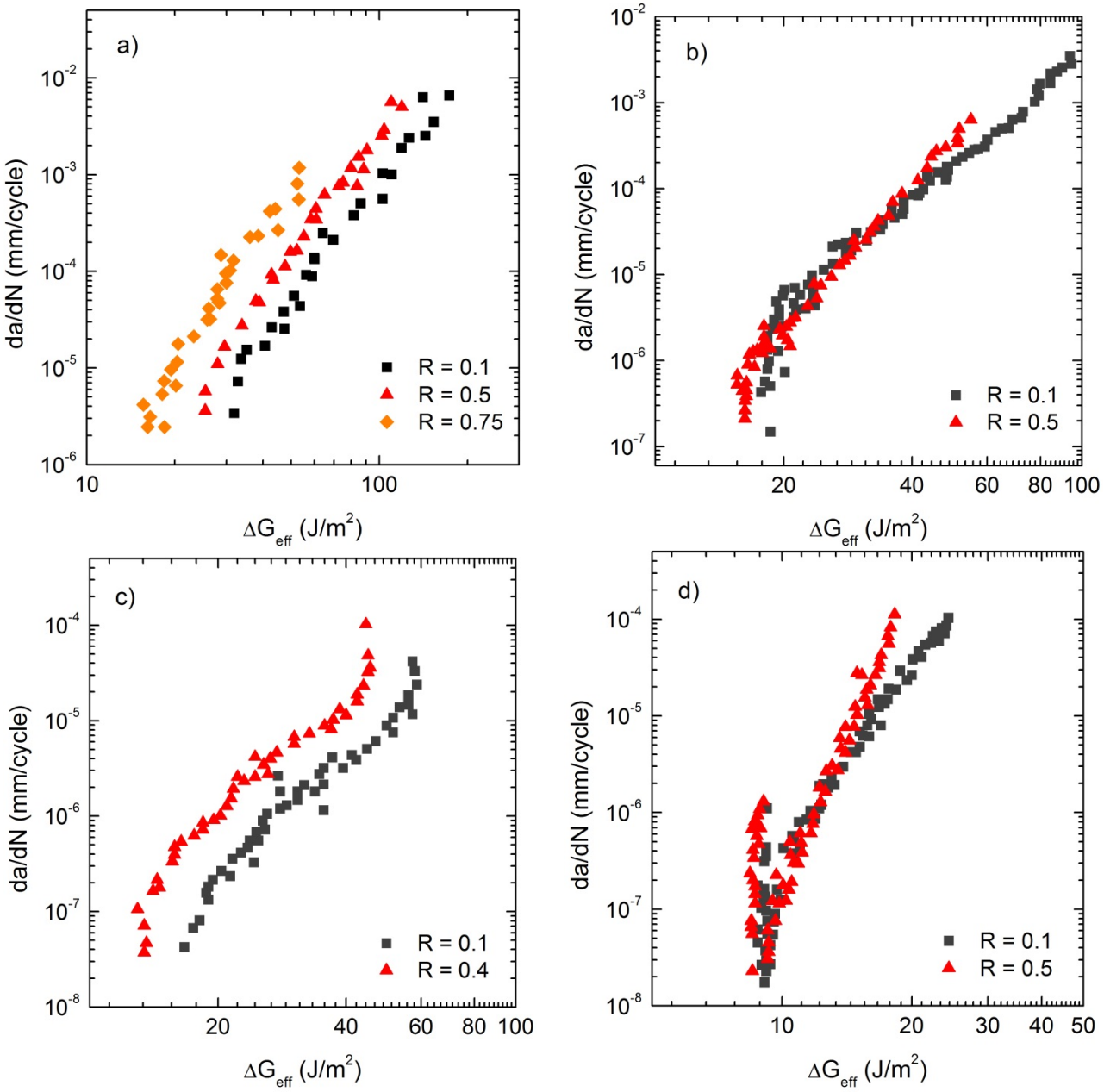

Figure 11 Mode I fatigue debonding results plotted using Forman's equation for (a) EC-3445 [5], (b) Cytec 4535A [7], (c) Multibond 330 [8] and (d) Toho 111 interleaved [4] adhesives.